BJP British Journal of Pharmacology

DOI:10.1111/bph.12102
www.brjpharmacol.org

RESEARCH PAPER

Inhibition of MAO-A and stimulation of behavioural activities in mice by the inactive prodrug form of the anti-influenza agent oseltamivir

Miki Hiasa[1], Yumiko Isoda[1], Yasushi Kishimoto[2], Kenta Saitoh[3], Yasuaki Kimura[3], Motomu Kanai[3], Masakatsu Shibasaki[4], Dai Hatakeyama[1], Yutaka Kirino[2] and Takashi Kuzuhara[1]

[1]*Laboratory of Biochemistry, Faculty of Pharmaceutical Sciences, Tokushima Bunri University, Tokushima, Japan,* [2]*Laboratory of Neurobiophysics, Kagawa School of Pharmaceutical Sciences, Tokushima Bunri University, Kagawa, Japan,* [3]*Graduate School of Pharmaceutical Sciences, The University of Tokyo, Tokyo, Japan, and* [4]*Institute of Microbial Chemistry, Tokyo, Japan*

Correspondence
Takashi Kuzuhara, Laboratory of Biochemistry, Faculty of Pharmaceutical Sciences, Tokushima Bunri University, Yamashiro-cho, Tokushima 770-8514, Japan. E-mail: kuzuhara@ph.bunri-u.ac.jp

The first three authors contributed equally to this work.

References from the FDA websites are supplied in Supporting Information.

Keywords
oseltamivir; monoamine oxidase; stimulated behaviour; prodrug

Received
12 October 2012
Revised
14 December 2012
Accepted
29 December 2012

BACKGROUND AND PURPOSE

Oseltamivir is the most widely prescribed anti-influenza medication. However, in rare instances, it has been reported to stimulate behavioural activities in adolescents. The goal of this study was to determine the molecular mechanism responsible for these behavioural activities.

EXPERIMENTAL APPROACH

We performed an *in vitro* assay of MAO-A, the enzyme responsible for neurotransmitter degradation, using either the active form – oseltamivir carboxylate (OC) or the inactive prodrug – oseltamivir ethyl ester (OEE). We also analysed the docking of MAO-A with OEE or OC *in silico*. Mouse behaviours after OEE or OC administration were monitored using automated video and computer analysis.

KEY RESULTS

OEE, but not OC, competitively and selectively inhibited human MAO-A. The estimated K_i value was comparable with the K_m values of native substrates of MAO-A. Docking simulations *in silico* based on the tertiary structure of MAO-A suggested that OEE could fit into the inner pocket of the enzyme. Behavioural monitoring using automated video analysis further revealed that OEE, not OC, significantly enhanced spontaneous behavioural activities in mice, such as jumping, rearing, sniffing, turning and walking.

CONCLUSIONS AND IMPLICATIONS

Our multilevel analyses suggested OEE to be the cause of the side effects associated with oseltamivir and revealed the molecular mechanism underlying the stimulated behaviours induced by oseltamivir in some circumstances.

Abbreviations

ALDH2, aldehyde dehydrogenase 2; AU, arbitrary unit; FDA, Food and Drug Administration; ICV, intracerebroventricular; OC, oseltamivir carboxylate (active form); OEE, oseltamivir ethyl ester (inactive prodrug)

Introduction

Ameliorating the side effects of clinically administered drugs is an important aspect of human health, even if the side effects occur rarely. Oseltamivir (Moscona, 2005; De Clercq, 2006; Jefferson *et al.*, 2006) exhibits potent antiviral activity against the influenza virus (Neumann *et al.*, 2009; Medina and García-Sastre, 2011), a virus that has caused more than 50 million deaths throughout human history. The drug primarily inhibits neuraminidase, an enzyme essential for the release of virions from infected cells. Oseltamivir is administered as an inactive prodrug in an ethyl ester form (oseltamivir ethyl ester, OEE), which is converted *in vivo* to its active carboxylate form (oseltamivir carboxylate, OC), as shown in Figure 1A–C (Abdel-Rahman *et al.*, 2011).

Since 1999, about 50 million people, of whom approximately 75% are Japanese, have been treated with oseltamivir; the possible adverse effects of this drug are therefore an important issue. In rare instances reported mainly in Japan, individuals receiving oseltamivir, who were typically under the age of 20 years, showed adverse psychological and neuropsychiatrical effects (Maxwell, 2007; Jefferson *et al.*, 2009; Kitching *et al.*, 2009; Nakamura *et al.*, 2010; L'Huillier *et al.*, 2011), such as dyskinaesia and depressive episodes (Chung and Joung, 2010; Kadowaki *et al.*, 2011). These effects have been compiled in documents published by the US Food and Drug Administration (FDA) (http://www.fda.gov/Safety/MedWatch/SafetyInformation/SafetyAlertsforHumanMedicalProducts/ucm095044.htm, UCM134319.pdf and UCM303004.pdf: URLs of other FDA information are shown in the Supporting Information). Reports of oseltamivir-related adverse events especially increased in 2009 when an influenza pandemic occurred and large amounts of this drug were prescribed (UCM303007.pdf), suggesting a correlation. However, the link between oseltamivir and neuropsychiatric adverse effects remains controversial, as several studies have shown that oseltamivir has no endogenous targets and causes no significant abnormal behaviour in humans (Toovey *et al.*, 2008; Lindemann *et al.*, 2010; Donner *et al.*, 2011). Moreover, a report published by the US FDA – UCM303008.pdf on the FDA website – concluded that there is no evidence for neuropsychiatric adverse effects of oseltamivir.

Studies have shown that oseltamivir crosses the blood–brain barrier in animals, including primates (Takashima *et al.*, 2011) and rats (Ose *et al.*, 2008; 2009; Hatori *et al.*, 2009; 2011; Oshima *et al.*, 2009; Takashima *et al.*, 2011); brain uptake is greater in younger versus older animals. OEE has been reported to have multiple effects on central nervous system function *in vivo* and *in vitro*: interaction with neurostimulants to alter synaptic plasticity or behaviour (Izumi *et al.*, 2008); neuroexcitation (Izumi *et al.*, 2007); enhancement of hippocampal network synchronization (Usami *et al.*, 2008); and interaction with alcohol (Izumi *et al.*, 2007), caffeine (Uchiyama *et al.*, 2010), and morphine (Crain and Shen, 2004) to affect neuronal activity. Oseltamivir also increases the level of dopamine in the rat cortex (Yoshino *et al.*, 2008; Guzmán *et al.*, 2010) and dopamine D2 agonist-mediated abnormal behaviour (Suzuki and Masuda, 2008); however, it does not alter the release or re-uptake of monoamines or GTP binding in postsynapses (Satoh *et al.*, 2007).

To elucidate the causal link between the mode of action of oseltamivir and its possible behavioural side effects, we aimed to identify its molecular target(s) of this drug. Neurotransmitters such as dopamine, norepinephrine and serotonin are metabolized by MAO as shown in Supporting Information Figure S1 (Youdim and Bakhle, 2006; Youdim *et al.*, 2006). Because mutations in the MAO-A gene have been reported to stimulate aggressive and anxiety-like behaviours in both humans and animals (Shih *et al.*, 1999; Caspi *et al.*, 2002; Chen *et al.*, 2004; Meyer *et al.*, 2006), we hypothesized that MAO is an endogenous target of oseltamivir. Therefore, we examined the effects of OEE and OC on MAO activity *in vitro*. We also investigated whether OEE and OC injected directly into the ventricles of the brain induces spontaneous behaviour *in vivo*.

Methods

Preparation of OEE and OC

Preparation and purification of OEE and OC (previously referred to as Ro 64-0802) are described in the Supporting Information. Both OEE and OC were dissolved in 50 mM Tris-HCl (pH 7.5), 100 mM NaCl, 5 mM $CaCl_2$ and 0.01% NP-40 for use in all experiments. To permit a direct comparison with OC and to eliminate an effect of phosphate, OEE was prepared in the phosphate-free form (Figure 1A).

MAO assay

MAO (EC 1.4.3.4) assays were performed using MAO-Glo™ assay reagent (Promega, Madison, WI) (Valley *et al.*, 2006), and are described in the Supporting Information. We defined one arbitrary unit (AU) to be the amount of reaction product generated from 1 μM substrate in the assay reactions. The linearity between the AUs and substrate concentrations was reproducible. Effects of OEE on MAO V_{max} and K_m were determined using Michaelis–Menten and Lineweaver–Burk analyses (Dixon and Webb, 1979). The K_i values of OEE for MAO were calculated using Dixon plot and slope–replot analyses as described previously (Dixon and Webb, 1979; Valley *et al.*, 2006).

In silico *docking simulation analysis of OEE with MAO-A or MAO-B*

Molecular modelling was performed using Molecular Operating Environment software (MOE; Chemical Computing Group, Quebec, Canada; Goto and Kataoka, 2008; Iwai *et al.*, 2011). The X-ray crystallographic structures of MAO-A (PDB ID codes: 2Z5X and 2Z5Y) and MAO-B (2XFQ) were obtained from a protein data bank (Son *et al.*, 2008; Bonivento *et al.*, 2010). The details are described in the Supporting Information. To evaluate this method, we confirmed the docking of MAO-A with serotonin, a known substrate, as shown in Supporting Information Figure S2.

Pharmacological treatments

The details of animals used in the behavioural study are described in the Supporting Information. Mice were anaesthetized with ketamine (80 $mg \cdot kg^{-1}$, i.p.; Daiichi Sankyo,

A

^{1}H NMR

OEE

inactive form

prodrug

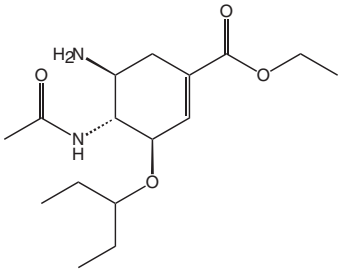

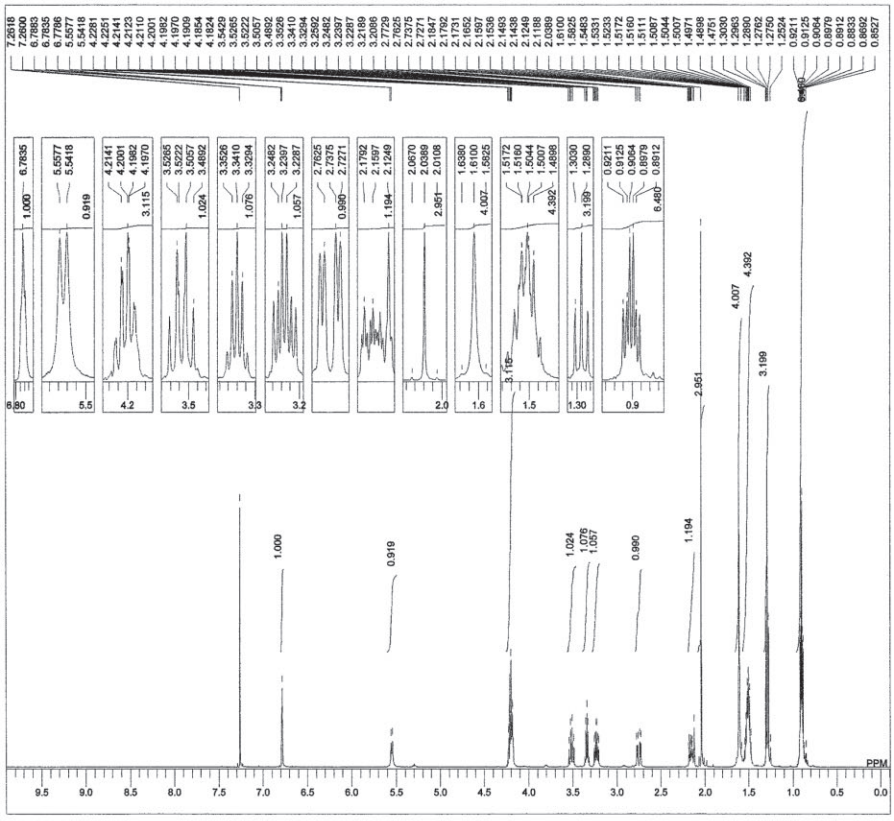

B

^{1}H NMR

OC

active form

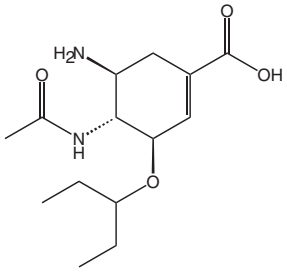

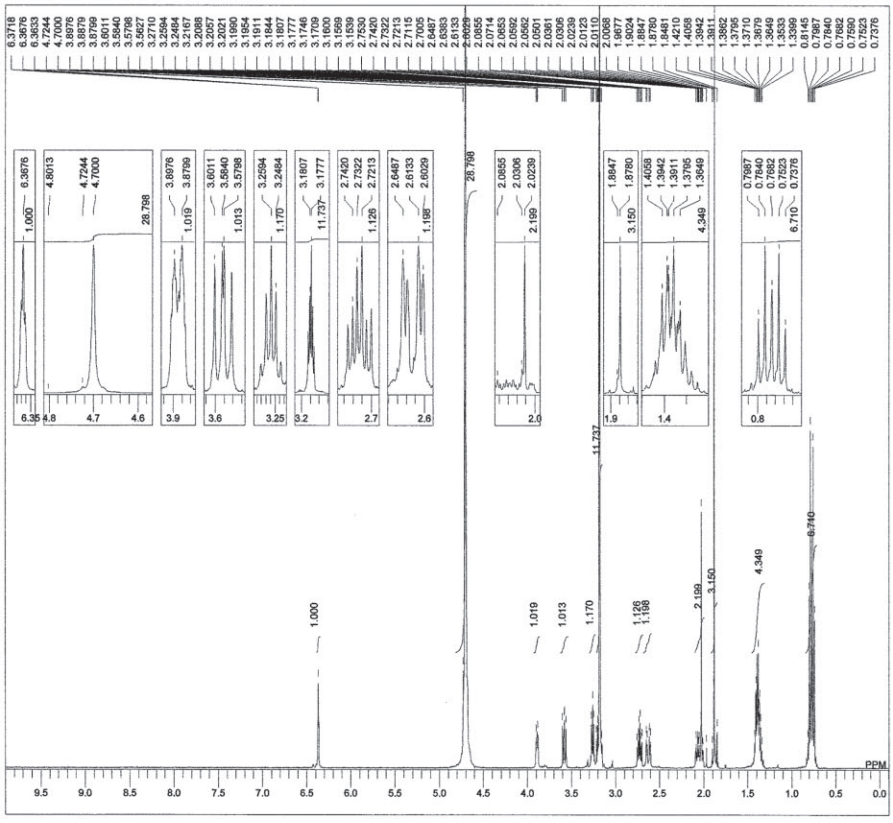

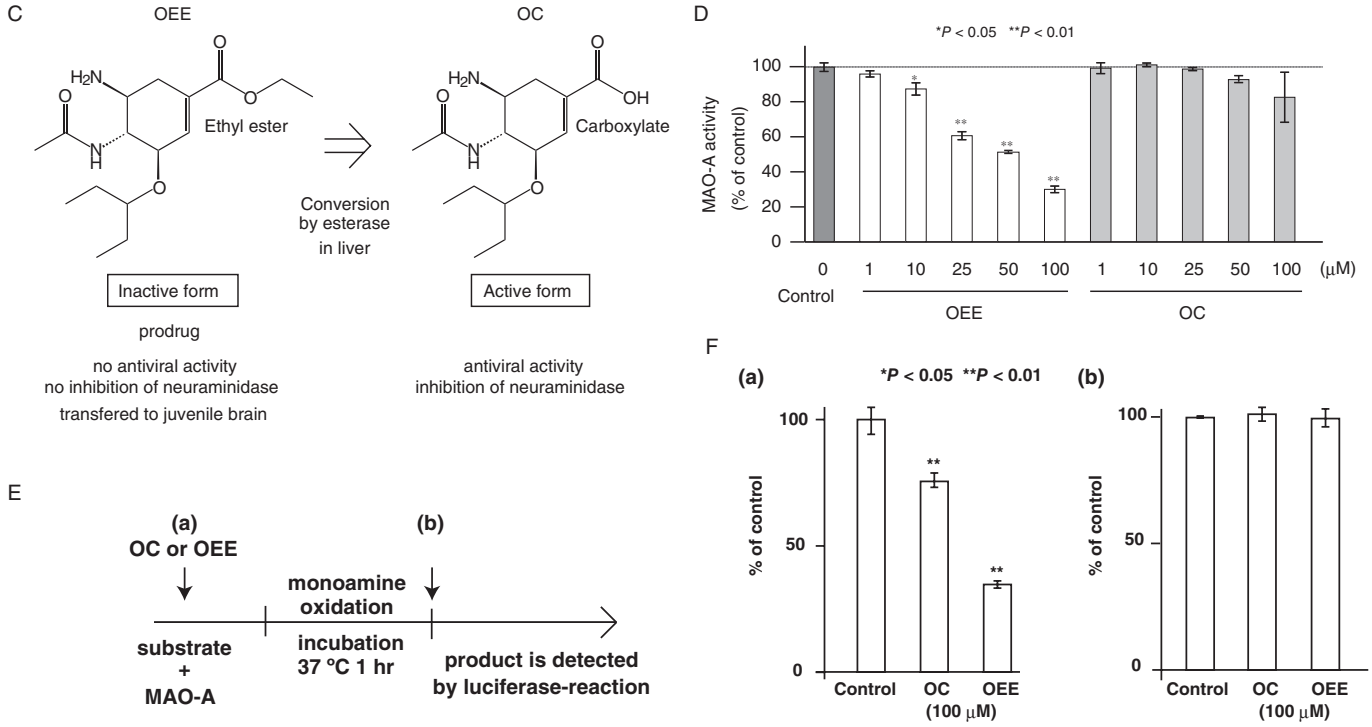

Figure 1

Inhibition of MAO-A by OEE, but not by OC. (A) Chemical structure and ^{1}H-NMR spectrum of the purified OEE. (B) Chemical structure and ^{1}H-NMR spectrum of the purified OC. (C) Conversion from the OEE to OC. OEE and OC harbour an ethyl ester residue and a carboxylic acid residue respectively. (D) MAO-A activity in the presence of OEE or OC. The vertical axis represents product formation (as a percentage of the control). MAO assays were performed in the absence (control) or presence of OEE or OC (1, 10, 25, 50 or 100 μM); assays were performed in triplicate. A 100% value equates to a luminescence reading of 2×10^6. (E) Schema of the experiment shown in (F). OEE or OC was added to the reaction either before (a) or after (b) the monoamine oxidation step. (F) Confirmation that MAO inhibition by the OEE is due to the targeting of monoamine oxidation. Panels (a) and (b) show the results of the effects on MAO by OEE or OC before or after the reaction respectively. The vertical axis represents product formation as a percentage of the control without inhibitor; assays were performed in triplicate. *$P < 0.05$, and **$P < 0.01$ (vs. the control). Data are presented as mean ± SD.

Tokyo, Japan) and xylazine (20 mg·kg^{-1}, i.p.; Bayer, Tokyo, Japan) and mounted in a stereotaxic instrument (David Kopf Instruments, Tujunga, CA, USA). Intracerebroventricular (ICV) injections were performed as described previously (Haley and McCormick, 1957). Briefly, mice were implanted with a single cannula (Plastic One, Roanoke, VA, USA) placed in the right lateral ventricle. The guide cannula (23 G) (Plastic One) was inserted stereotaxically into the cerebral ventricle at positions –0.2 mm anteroposteriorly, 1.1 mm right, and –2.0 mm dorsoventrally from the bregma. The cannulas were fixed to the skull using three 7 mm stainless steel screws and dental cement. Animals were allowed to recover from surgery for at least 5 days before behavioural testing, during which time 30-G dummy cannulas were left inside the guide cannula. ICV infusions were then performed using 30-G cannulas that were cut to extend 1.0 mm beyond the end of the guide cannula. The dummy cannulas were removed and replaced with infusion cannulas that were connected to 5 μL syringes. OEE or OC (1.5 or 5 nmol per mouse) or vehicle solution (125 mM NaCl, 3.8 mM KCl, 2.0 mM $CaCl_2$, 1.0 mM $MgCl_2$, 1.2 mM KH_2PO_4, 26 mM $NaHCO_3$ and 10 mM glucose) was subsequently injected through the infusion cannulas (5 μL, respectively). Dose selection was based on (i) allometric translation of the dose administered to humans – 70 mg·day^{-1}, or 1 mg·kg^{-1}, which is comparable with 580 μg per mouse (40 g) or 1.8 μmol per mouse by the body surface method (Reagan-Shaw *et al.*, 2008) and (ii) doses previously reported in the literature – 50 mg·kg^{-1}, or 6.4 μmol per mouse (assuming body weight of 40 g) administered by intraperitoneal administration (Izumi *et al.*, 2007; 2008).

Behavioural analysis of the mice: automated video analysis of spontaneous physical activities in the cage

Behavioural tests were conducted in mice at the age of 12–16 weeks, as previously described (Roughan *et al.*, 2009; Kishimoto *et al.*, 2013). Briefly, we used a digital video-based analysis system, HomeCageScan (HCS, Clever Systems, Inc., Reston, VA, USA), which automatically detected, recorded, categorized and quantified mouse behaviour. After drug treatment, each mouse was immediately placed in a clear cage (21 × 31 × 12 cm), and the spontaneous physical activities of these animals were recorded for 1 h in the home cage using a standard digital camcorder (NV-GS300, Panasonic, Osaka, Japan), which was mounted on tripods angled perpendicular to the cage to provide a side view. The camera footage was

electronically stored using mAgicTV software (I-O DATA, Ishikawa, Japan). The video movie data were analysed using HCS. Spontaneous behaviours, including locomotor activity, rearing and hanging, were evaluated automatically.

Statistical analysis

The data were analysed by Student's *t*-test or one-way ANOVA. *Post hoc* analysis of the differences between oseltamivir-treated groups and control subjects was performed using Dunnett's test. Differences were considered significant at $P < 0.05$.

Results

Selective inhibition of MAO-A by OEE in vitro

To exclude any possible effects of impurities in the preparations of these compounds, OEE and OC were purified as described previously, and analysed by ^{1}H-NMR (500 MHz; Figure 1A and B). All resonance spectra in ^{1}H-NMR analysis were assigned to their structures of OEE and OC (Figure 1A and B), indicating that the purities of OEE and OC were >95%.

There are two isoforms of MAO, MAO-A and MAO-B (Youdim and Bakhle, 2006; Youdim *et al.*, 2006), both of which are expressed in neurons and astrocytes, although they have different functional roles. MAO-A degrades dopamine, serotonin, melatonin, norepinephrine and epinephrine, whereas MAO-B targets dopamine and phenethylamine (Supporting Information Figure S1). We first tested whether OEE or OC inhibits MAO-A using a human MAO-A assay (Valley *et al.*, 2006) as depicted in Figure 1C. Figure 1D shows that OEE caused dose-dependent inhibition of MAO-A at concentrations of ≥10 μM ($P < 0.05$); conversely, OC had no effect. These findings suggest that OEE, but not OC, has the capacity to exert behavioural effects, and that the ethyl ester group of OEE is important for the inhibitory effects on MAO-A (Figure 1C, D). To confirm these findings, we added OEE or OC before or after a monoamine oxidation reaction (Figure 1E). Addition of OEE prior to, but not after, monoamine oxidation decreased the product levels (Figure 1F). These data, rather than the detection steps in the assay, suggest that OEE inhibits monoamine oxidation per se.

We next tested whether OEE also inhibits MAO-B. OEE up to a concentration of 100 μM had no effect on MAO-B (150 μU) activity; rather, it caused slight stimulation (Figure 2A). OEE (100 μM) also had no effect on lower doses (40, 80 or 160 μU) of MAO-B (Figure 2B). These results indicate that OEE selectively inhibits MAO-A. Because mutations in MAO-A have been associated with some types of abnormal

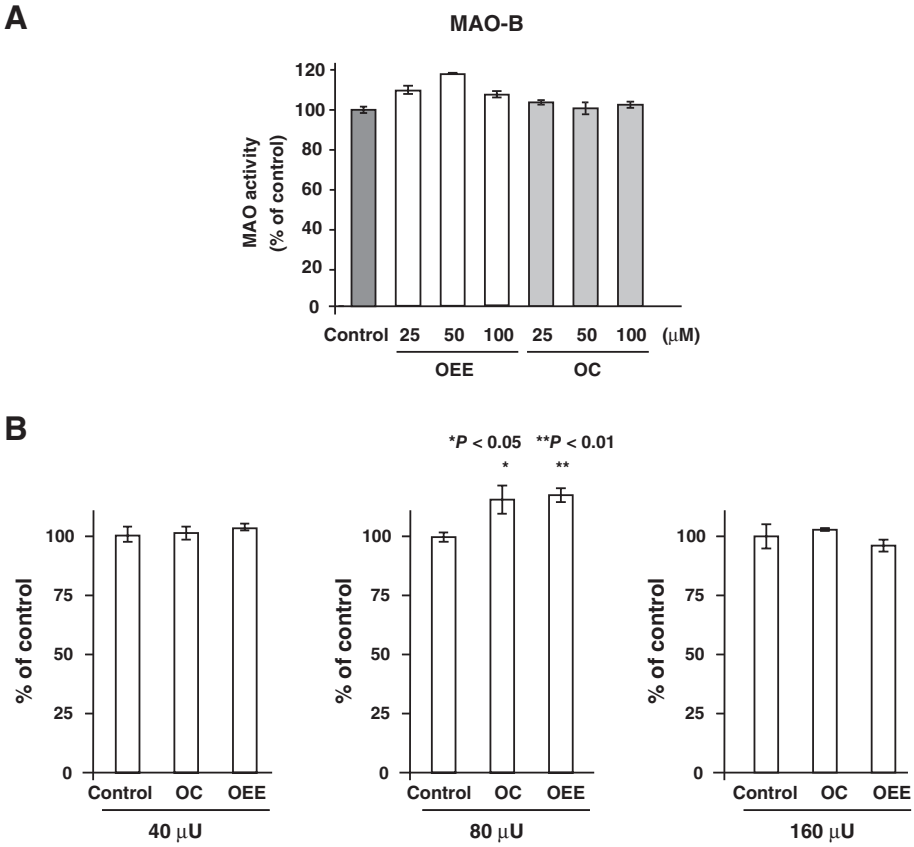

Figure 2

Effect of OEE on MAO-B. (A) The activity of MAO-B (160 μU) was assayed in the absence or presence of OEE or OC (1, 10, 25, 50 or 100 μM). The vertical axis indicates product formation (as a percentage of the control without inhibitor). (B) OEE (100 μM) does not inhibit any activities (40, 80 or 160 μU) of MAO-B. Assays were performed in triplicate. Data are presented as mean ± SD.

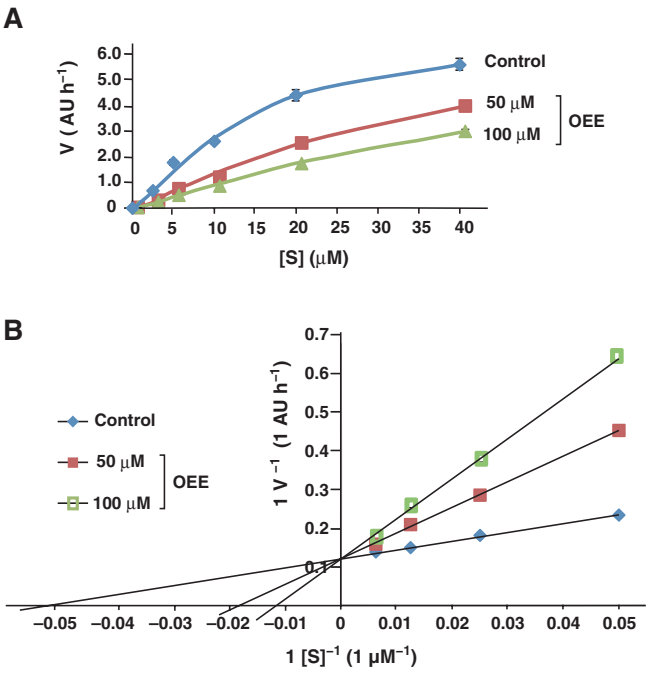

Figure 3

Competitive inhibition of MAO-A by OEE. (A) Dose–response curves indicating that inhibition of MAO-A by OEE follows Michaelis–Menten kinetics. MAO-A assay was performed in the absence or presence of OEE (50 or 100 μM) with MAO-A substrate (0, 2.5, 5, 10, 20 or 40 μM). (B) Lineweaver–Burk plot analysis. MAO-A assay was performed in the absence or presence of OEE (50 or 100 μM) with MAO-A substrate (0, 20, 40, 80 or 1600 μM). Assays in (A) and (B) were performed in triplicate. Data are presented as mean ± SD.

behaviour (Shih *et al.*, 1999; Caspi *et al.*, 2002; Chen *et al.*, 2004; Meyer *et al.*, 2006), this result is consistent with the manifestation of the stimulated behaviour in some individuals who have been treated with oseltamivir.

Competitive inhibition of MAO-A by OEE

To investigate the mechanism by which OEE inhibits human MAO-A, we constructed Michaelis–Menten and Lineweaver–Burk plots (Dixon and Webb, 1979) from the results of MAO-A assays. At a low range of substrate concentration (0–40 μM), MAO-A followed Michaelis–Menten kinetics in the absence or presence (50 or 100 μM) of OEE; OEE inhibited MAO-A at all substrate concentrations (Figure 3A). We then generated a Lineweaver–Burk plot from an MAO assay using a higher range of substrate concentrations (0–160 μM) (Figure 3B): at 0 μM OEE (control), V_{max}: 8.2 (AU·h^{-1}), K_m: 18 (μM); at 50 μM OEE, V_{max}: 8.2 (AU·h^{-1}), K_m: 56 (μM); at 100 μM OEE, V_{max}: 10.1 (AU·h^{-1}), K_m: 111 (μM). The V_{max} values (Y-intercepts) were similar, whereas the K_m values (X-intercepts) markedly differed at each concentration of OEE (Figure 3B), suggesting that OEE competitively inhibits MAO-A.

In silico *modelling*

To test the hypothesis that the competitive inhibition of MAO-A by OEE involves the binding of OEE to the active pocket of the enzyme, we performed *in silico* docking simulation analysis (Goto and Kataoka, 2008; Iwai *et al.*, 2011) using both OEE and OC. The crystal structure of the complex of human MAO-A with harmine, a known MAO-A inhibitor, has already been reported (Son *et al.*, 2008), providing valuable tertiary structure information for this analysis. The results showed that OEE binds deep within the narrow pocket that forms the active site; binding occurs via hydrophobic interactions between the ethyl ester group of OEE and MAO-A (Figure 4A, B). The binding site of OEE was near the flavin group of flavin adenine dinucleotide (Figure 4A, B). The binding position of OEE was found to be almost similar to that of harmine, which is also known to interact with the substrate-binding site (Figure 4A, C). This is consistent with the results shown in Figure 3B, which indicate the competitive nature of MAO-A inhibition by OEE. Because MAO catalyses its reactions using the flavin group, we conclude that OEE inhibits monoamine oxidation by disrupting its interaction with this moiety. Docking simulation of OC with human MAO-A revealed that its carboxyl group is positioned towards the entrance of the pocket and that the hydrophobic interaction via the ethyl ester group is lost (Figure 4D, E). The binding energy of OEE (–8.3 kcal·mol^{-1}) was lower than that of OC (–7.1 kcal·mol^{-1}), suggesting that a more stable interaction occurs between OEE and MAO-A. Taken together, these data reveal mechanistically why OEE can inhibit MAO-A, whereas OC has negligible effects.

From the viewpoint of medicinal chemistry, we compared the chemical structures of OEE and known MAO-A and MAO-B inhibitors (Figure 4F) that have been used to treat depression or Parkinson's disease (Youdim and Bakhle, 2006; Youdim *et al.*, 2006). MAO-A inhibitors harbour an amine group (indicated in red), an ethyl group followed by an amine group (indicated in cyan), and a bulky hydrophobic group that includes a double bond-like phenyl group near ethylamine (shown in green) (Figure 4F). Oseltamivir does not have a phenyl group, but does contain a bulky hydrophobic group including a double bond (Figure 4F). Therefore, these common structures might be important for the inhibitory activity of these agents against MAO-A. Furthermore, the OEE-specific ethyl ester group forms a bulky hydrophobic group (Figure 4F), again indicating the importance of this moiety for the inhibition of MAO-A.

We also performed docking simulation analysis using MAO-B (Youdim and Bakhle, 2006). Tertiary structural analyses of the human MAO-A and MAO-B have revealed that although the primary structures of the two proteins are similar, human MAO-A exists as a monomer, while MAO-B adopts a dimeric conformation (Youdim and Bakhle, 2006; Youdim *et al.*, 2006). The cavities of the enzyme pockets of MAO-A and MAO-B have also been reported to differ (Youdim *et al.*, 2006). In our current *in silico* analysis, even the most stable binding result indicated that OEE might bind to the outer surface of the MAO-B protein (Figure 5A, B). The binding energy in this case was –5.0 kcal·mol^{-1} (Figure 5C), which is higher than that recorded for MAO-A (–8.3 kcal·mol^{-1}; Figure 4D). This result thus provides a mechanistic underpinning to the selectivity of OEE for MAO-A.

Estimation of the K_i of OEE toward MAO-A

To determine the concentration of OEE that is effective in inhibiting MAO-A, we estimated its K_i using Dixon plot and

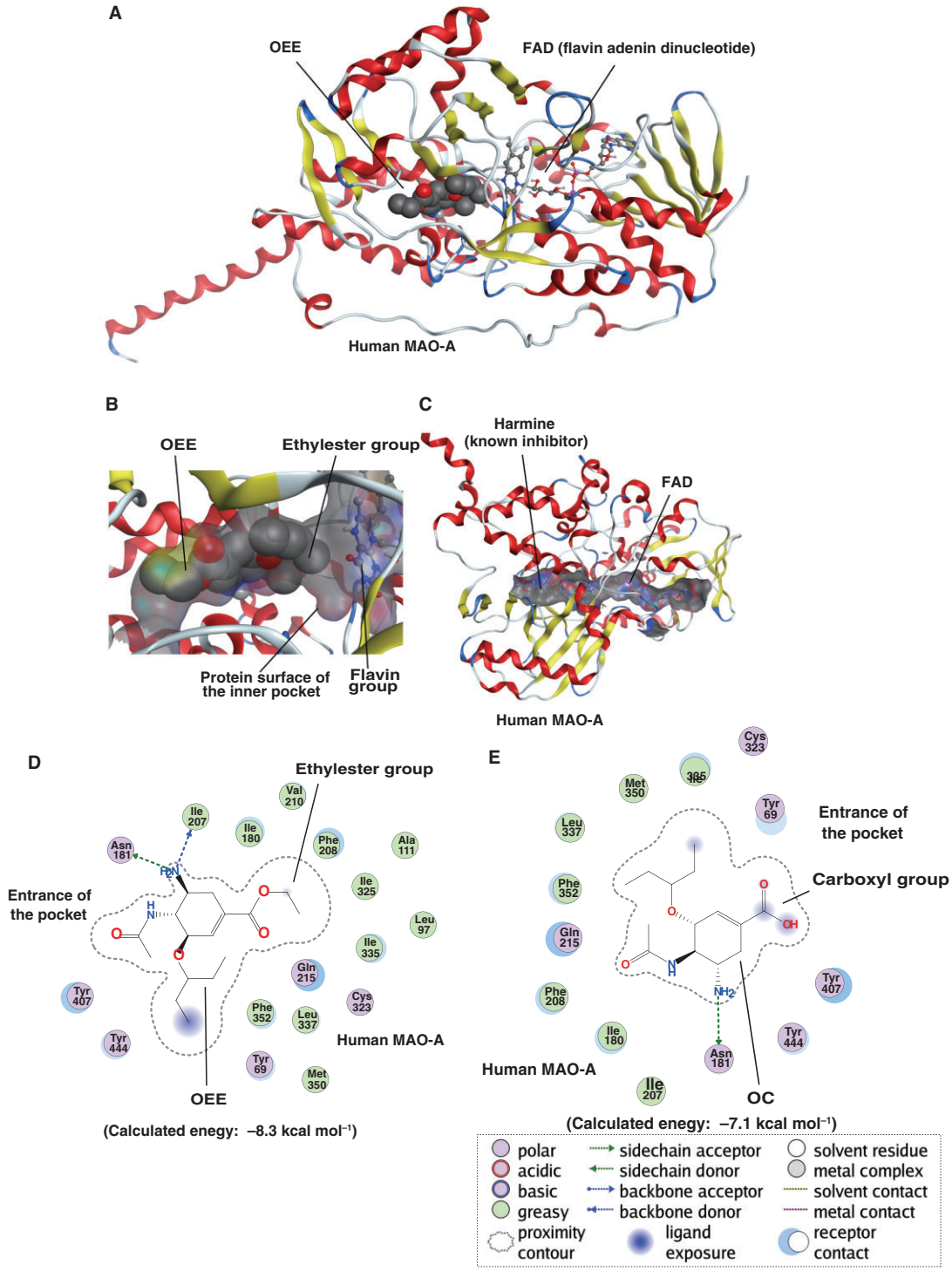

Figure 4

In silico docking simulation of OEE and OC with MAO-A. (A) The α-helix and β-strands of MAO-A are indicated in red and yellow respectively. OEE is shown here as a ligand. (B) Fitting of OEE to the active pocket of MAO-A. Oseltamivir is displayed in a ball-stick mode. The surface of the pocket of MAO-A is highlighted. (C) Crystal structure of the complex of MAO-A and harmine, a reversible inhibitor of MAO-A. The tertiary structure of the complex was developed using the MOE program. (D, E) *In silico* two-dimensional analysis of the interaction between OEE (D) or OC (E) forms of oseltamivir and human MAO-A. The chemical structure of OEE is shown in the centre with the key interacting amino acids depicted around it. The ethyl ester group of OEE interacts with the pocket of MAO-A. The amino acids and their numbers are indicated. The modes of the interactions are shown under each panel. (F) Comparison of the chemical structures of known MAO inhibitors and OEE. Amine groups are shown in red. Ethyl groups followed by an amine group are shown in cyan. Bulky hydrophobic groups including double bond-like phenyl groups near an ethylamine are depicted in green.

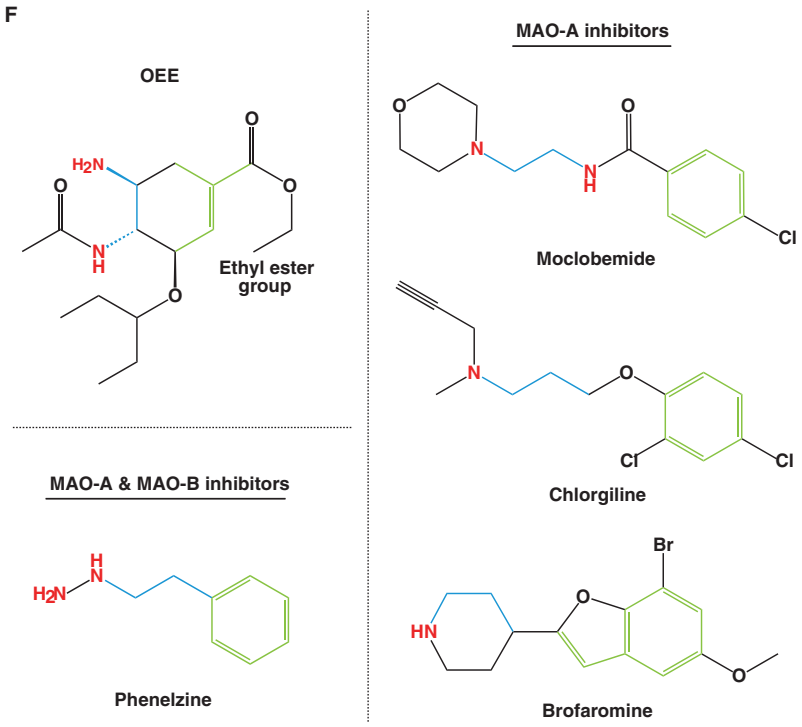

Figure 4

Continued

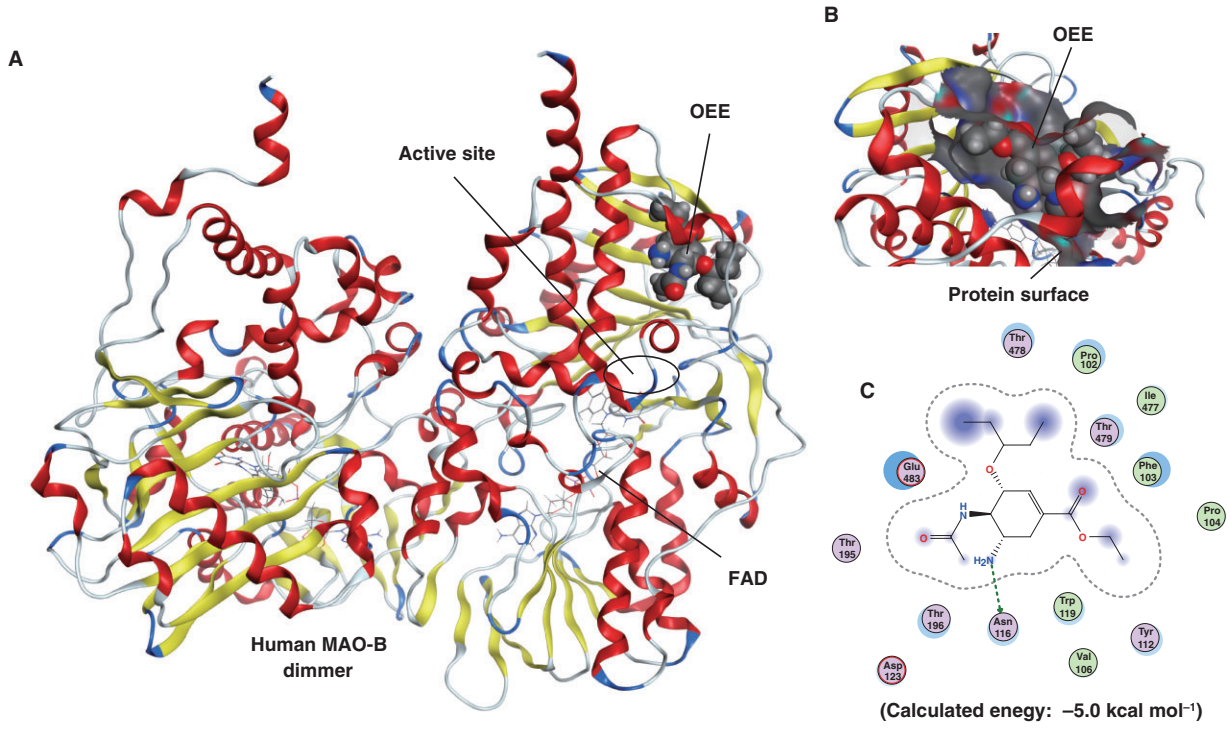

Figure 5

In silico docking simulation of OEE and OC with MAO-B. (A) The α-helix and β-strands of MAO-B (depicted in a ribbon structure) are shown in red and yellow, respectively. (B) Fitting of OEE to the active pocket of MAO-B. Oseltamivir is displayed in a ball and stick mode. The surface of the pocket of MAO-B is indicated. (C) Two-dimensional analysis of the interaction between OEE and MAO-B. The chemical structure of OEE is shown in the centre with the key interacting amino acids shown around it. The modes of the interactions are as shown for Figure 4D and E.

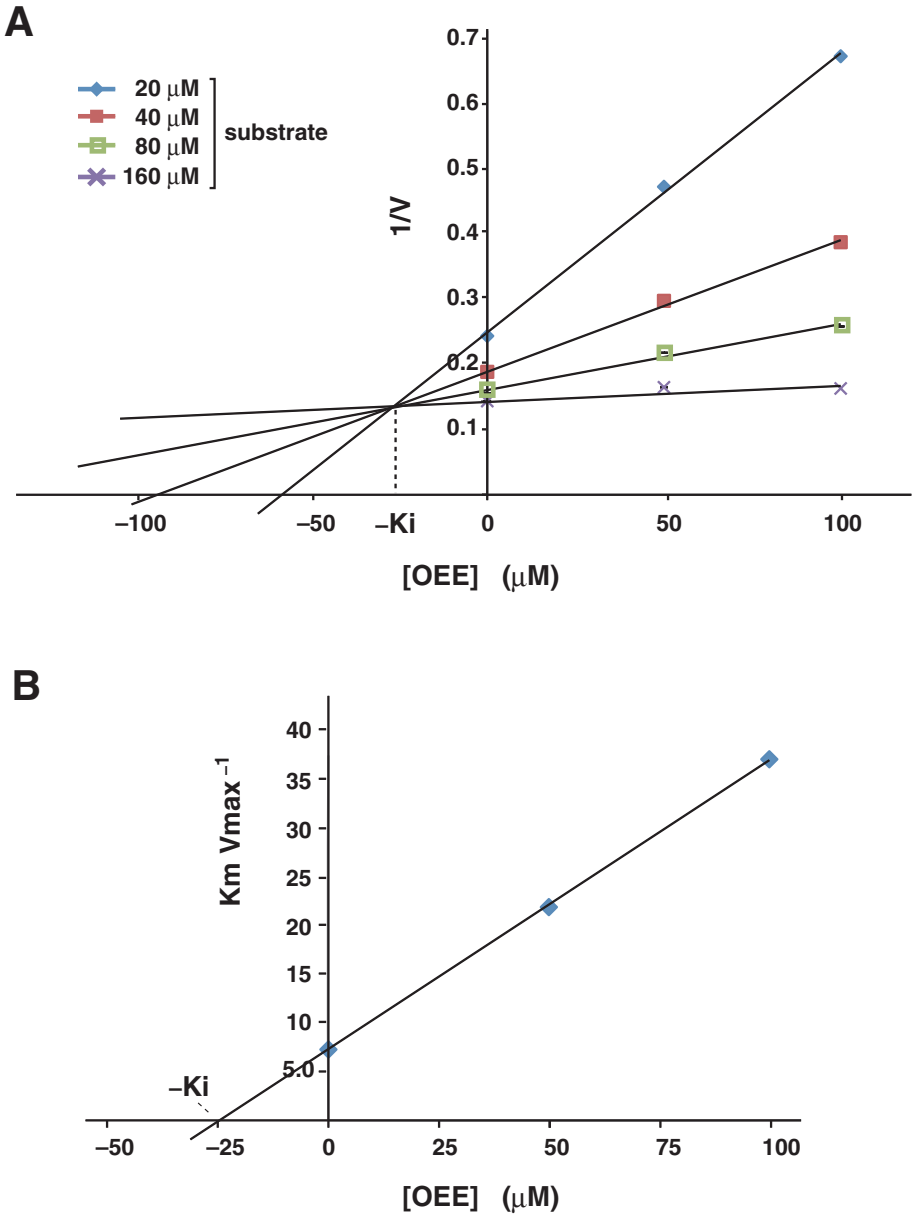

Figure 6

Estimation of the K_i of OEE against MAO-A. (A) Dixon plot analysis. MAO-A assay was performed in the absence or presence of OEE (50 or 100 μM) with MAO substrate (0, 20, 40, 80 or 160 μM). At the intersection point, the concentration of substrate indicates the $-K_i$ value, estimated at 25 μM in this analysis. (B) Slope-replot analysis. In this plot, the X-intercept indicates the $-K_i$ value, estimated at 28 μM as shown.

slope–replot analyses (Dixon and Webb, 1979; Kamal *et al.*, 2000). Analysis of the Dixon plot of a MAO-A assay using 20, 40, 80 or 160 μM of substrate, and 0, 50 or 100 μM of OEE revealed an estimated K_i value of 28 μM (Figure 6A); slope–replot analysis revealed an estimated K_i value of 25 μM (Figure 6B). Because the K_m values of serotonin and dopamine, determined using the same methods that we used here, were reported to be 45 and 21 μM, respectively (Supporting Information Table S1; Valley *et al.*, 2006), the K_i value of OEE can be considered effective.

Stimulation of mouse behaviour by OEE, but not OC

To investigate whether OEE specifically induces spontaneous behaviour *in vivo*, we performed *in vivo* behaviour analysis on mice administered OEE or OC by ICV injection using a computer-based behavioural analysis system (Roughan *et al.*, 2009; HCS, Supporting Information Figure S3). Typical examples of computer-based analysis of mouse behaviours are shown in Supporting Information movies. OEE, but not OC,

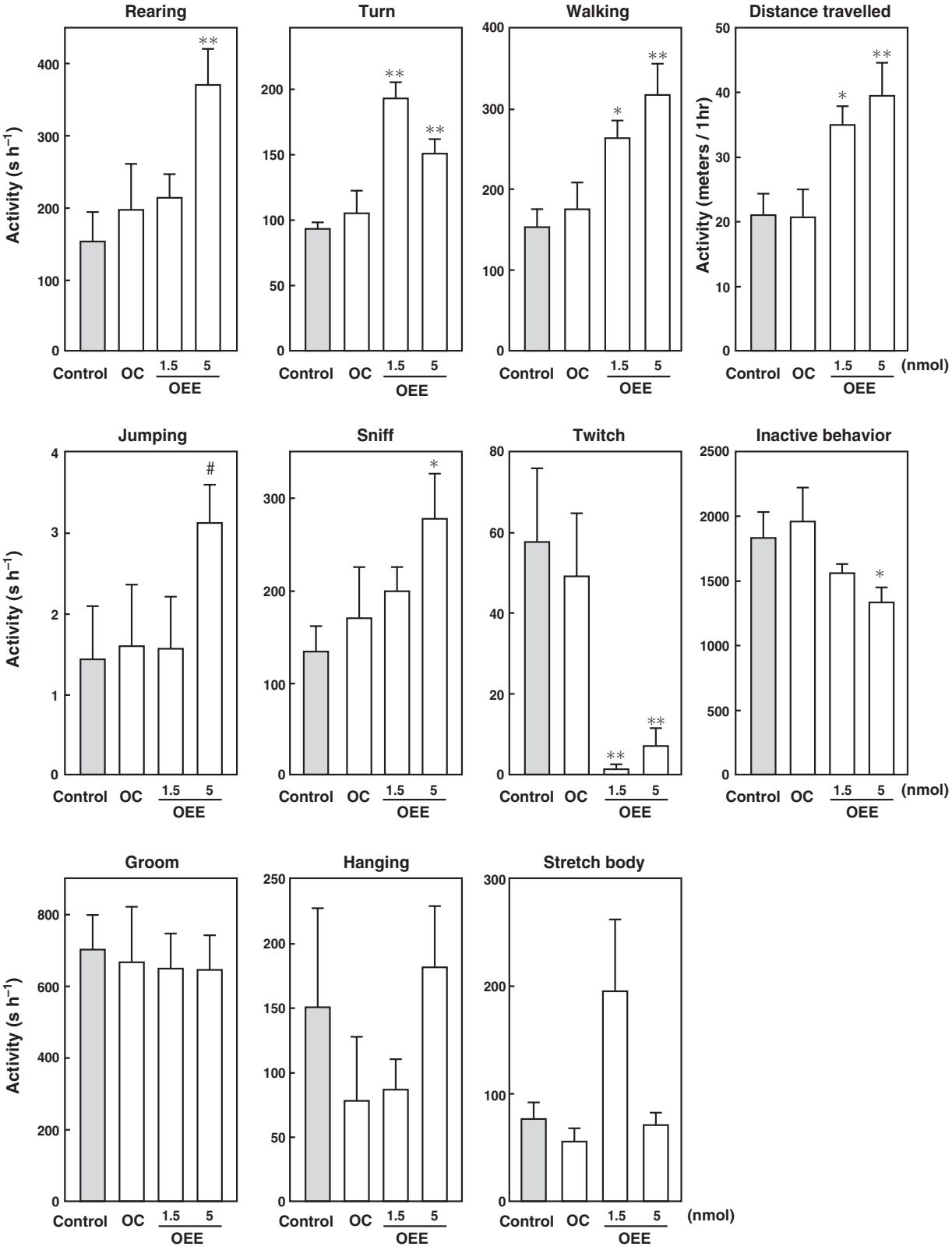

Figure 7

Behavioural analysis of OEE-injected mice *in vivo*. Behaviours of mice injected with vehicle (control, $n = 9$), 1.5 or 5 nmol of OEE ($n = 9$ or 11), or 5 nmol of OC ($n = 9$) were recorded and analysed using the HomeCageScan system. The vertical axes indicate the times of behaviours per hour ($s \cdot h^{-1}$), the distance travelled ($m \cdot h^{-1}$), or the period of inactivity ($s \cdot h^{-1}$). $^{\#}P < 0.05$ (vs. the control group) by Student's *t*-test; $^{*}P < 0.05$, and $^{**}P < 0.01$ (vs. the corresponding control group) by *post hoc* Dunnett's test. Data are represented as mean ± SEM.

induced increased 'rearing', 'turning', 'walking', 'jumping' and 'sniffing' by the animals (Figure 7 and Supporting Information Movies). OEE also increased 'distances travelled' by almost twofold of those in control mice, and significantly decreased 'twitching' and 'inactive behaviours' such as pausing, remaining low, sleeping, and the lengths of time in a stationary position (Figure 7). In contrast, 'grooming', 'hanging' and 'stretching' were not affected (Figure 7). Increases in 'walking' and 'distance travelled', basal barometers, were dose-dependent, while 'rearing', 'jumping' and 'sniffing' increased only at the 5 nmol dose. This may be due to differences in the sensitivities to OEE. In contrast, the 'inactive behaviour' parameter showed a tendency towards a dose-dependent decrease. This is the first demonstration of stimulation of mouse behavioural activities by OEE. These effects are consistent with our *in vitro* biochemical and *in silico* docking results.

Discussion

A working model

This is the first report to reveal the molecular target of oseltamivir, and thereby the first to provide an explanation for its behavioural effects. On the basis of our current data and previously reported results, we have devised a working model illustrated schematically in Figure 8 to explain the rare occurrence of stimulated behaviour in young people receiving oseltamivir. In almost all individuals, OEE was converted to OC by carboxylesterase 1A1 (HCE1) in the liver (Zhu and Markowitz, 2009; Zhu *et al.*, 2009; Abdel-Rahman *et al.*, 2011; Tarkiainen *et al.*, 2012; Figures 1C and 8), with no impact on MAO-A activity (Figure 1D) and thus no adverse effects (Figure 8). However, if this conversion does not occur or is inefficient, as has been shown in juvenile rat livers (Ose *et al.*,

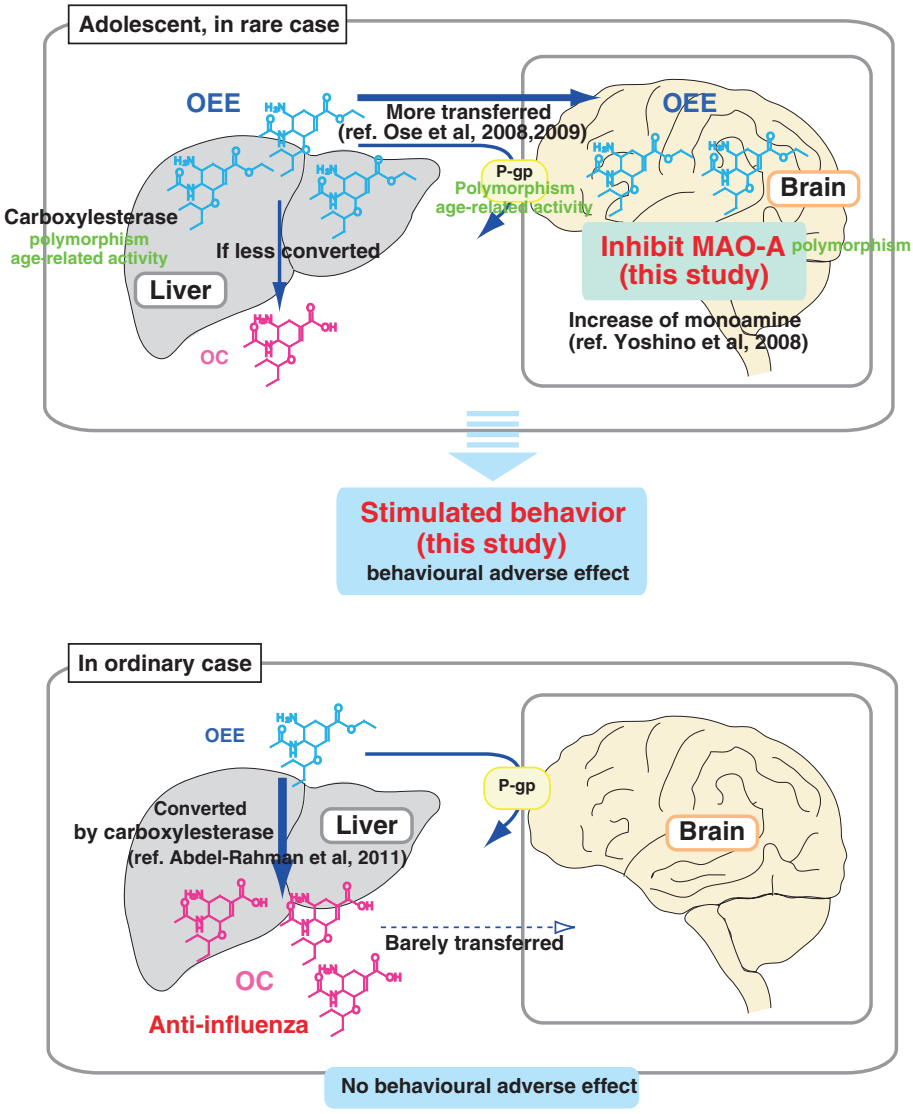

Figure 8

Proposed model for the effects of OEE on MAO-A and the resulting behavioural impact in humans. P-gp: P-glycoprotein.

2008), the concentration of OEE will increase in the bloodstream (Figure 8). Zhu *et al*. (2009) reported that the expression and the activity of human carboxylesterase 1 increase in an age-dependent manner. Impairment of the bioactivation of OEE by a carboxylesterase 1 polymorphism and side effects of OEE in a patient with liver cirrhosis have also been reported (Kaji *et al*., 2005; Zhu and Markowitz, 2009; Tarkiainen *et al*., 2012). Moreover, oseltamivir has been reported to affect liver function (El-Sayed and Al-Kahtani, 2011). Together, these results support our model by providing a possible explanation for the rare occurrence of adverse effects.

Role of the blood–brain barrier in our working model

Another consideration from our working model is the nature of the transfer of OEE into the brain as a function of age or disease state. L'Huillier *et al*. (2011) have reported that a human polymorphism in *ABCB1*, the gene that encodes P-glycoprotein at the blood–brain barrier, is associated with oseltamivir-related neuropsychiatrical adverse effects in children and young adults, indicating that the blood–brain barrier is important for the effect in these age groups (Figure 8). Other studies have shown that OEE accumulates in the juvenile rat brain at a higher level than OC does, because of the difference in the preference for P-glycoprotein (Ose *et al*., 2008; 2009; Figure 8). Moreover, Freichel *et al*. (2012) reported that the concentration of OEE in the brain is higher than that of OC, although these measurements in the plasma are controversial. The finding that the brain concentrations of OEE and OC increased in the presence of inflammation (Oshima *et al*., 2009), which can be induced by the influenza virus, is consistent with the observation that severe influenza causes hyperpermeability in the brain (Wang *et al*., 2010). Co-morbidity with influenza encephalopathy has also been described (UCM303007.pdf in FDA web site). Thus, if the blood–brain barrier is perturbed by influenza encephalopathy, OEE could more effectively distribute the brain (Figure 8).

Our working model is thus consistent with the current body of evidence and provides a plausible explanation as to why OEE has adverse effects in only some instances and only in children and adolescents. Moreover, the claims that oseltamivir is safe overall and that it has neuropsychiatrical activity in rare cases are not contradicted in our model. It is likely that most people can continue to safely use oseltamivir, but awareness of the possible, albeit rare, side effects of this drug in individuals who may have a metabolic or blood–brain barrier condition would be prudent.

Higher incidence of OEE behavioural side effects in Japanese

Sabol *et al*. (1998) reported that 33% of white/non-Hispanic individuals and 61% of Asians/Pacific islanders show low activity of the MAO-A promoter variant. This suggests there are ethnic differences in the sensitivity to MAO inhibitors, which may explain differences in the incidence of adverse effects of oseltamivir in different races. Furthermore, synergistic effects of oseltamivir with alcohol on neuronal function have been reported (Izumi *et al*., 2007). Metabolites of monoamine generated by the activity of MAO are further metabolized by aldehyde dehydrogenase (ALDH; Supporting Information Figure S1), which also degrades alcohol. Our current results provide an explanation for the molecular mechanism underlying this synergy. Approximately, 40% of the Japanese population lacks or is heterozygous for ALDH2, which is expressed in the brain and other tissues (Supporting Information Figure S1) (Crabb *et al*., 2004). The inhibition of MAO-A by OEE coupled with an ALDH2 deficiency might induce synergistic effects on this pathway in Japanese patients (Supporting Information Figure S1). Because many teenagers do not consume alcohol, it is also possible that their ALDH is not induced *in vivo* and is therefore maintained at lower levels than in adults. Together, these may explain why the side effects of oseltamivir are observed mainly in younger Japanese patients (Supporting Information Figure S1).

Concentration aspects

Recently, Freichel *et al*. (2012) reported that the average concentrations of oseltamivir in cerebrospinal fluid and in the brains of healthy rats reached 1120 $ng \cdot mL^{-1}$ (3.6 μM) and 2310 $ng \cdot g^{-1}$ (7.4 μM), respectively. ^{11}C-labelled oseltamivir analyses showed that oseltamivir is strictly localized in the infant brain; high levels were especially noted in the pineal body, (Hatori *et al*., 2011; Takashima *et al*., 2011), which produces melatonin, a substrate of MAO-A. Thus, accumulation of oseltamivir such that it approaches the Ki concentration of MAO-A may elicit more potent effects on MAO-A in this region. Furthermore, Toovey *et al*. have previously simulated the inhibition of the conversion of OEE to OC and found that it leads to a 14-fold higher concentration of OEE (Toovey *et al*., 2008).

Behavioural analysis

The stimulated behaviours in mice are consistent with the neuropsychiatric adverse effects in humans following oseltamivir administration. The increased distance travelled by mice because of OEE in the present study seems to mimic the stimulation of running in humans. Furthermore, in clinical cases, mood disorders associated with oseltamivir have been reported (UCM303006.pdf in FDA website), further suggesting an association, since mood is related to the actions of MAO.

Subcutaneous (s.c.) administration of 1–4 $mg \cdot kg^{-1}$ of amphetamine – a known inhibitor of MAO-A – stimulates spontaneous behaviours in mice in a dose-dependent manner (Hirabayashi *et al*., 1979). Another study has demonstrated that amphetamine (2.5 $mg \cdot kg^{-1}$, s.c.) induces enhanced locomotor activity in mice, whereas mice administered doses of amphetamines greater than 5 $mg \cdot kg^{-1}$ exhibit significant stereotypy (McNamara *et al*., 2006). Although the methods of administration and the dosages were unrelated, these findings are consistent with those reported in the present study.

Additional targets

Moclobemide is a reversible MAO-A inhibitor showing antidepressant activity. Moclobemide has almost no effect on spontaneous behaviour in mice, although a slight impairment in motor performance is seen at higher doses only (Burkard *et al*., 1989). Hence, we contend that the mecha-

nism of action of oseltamivir might not be fully equivalent to that of MAO-A inhibitors such as moclobemide. Oseltamivir has been reported to induce depressive episodes in humans (Chung and Joung, 2010). Although this seems contrary to its MAO-A inhibition profile, because brain functions are regulated by a fine balance of monoamines, we believe that this is not so. For example, the role of the MAO-A gene in bipolar affective disorder has been reported (Furlong *et al.*, 1999). However, this suggests that there may be additional targets that influence behaviour in humans, although Satoh *et al.* (2007) showed that neither Tamiflu nor GS4071 (OC) influence the re-uptake or release of monoamines in postsynapses. As indicated by our current findings, there are structural similarities among oseltamivir and monoamines (Figure 2H). Hence, OEE may possibly block or stimulate the other monoamine machineries.

Conclusions

We conclude that OEE, but not OC is responsible for the occasionally observed behavioural side effects of oseltamivir and that MAO-A is one of the important targets. The finding that OC does not inhibit human endogenous neuraminidases (Hata *et al.*, 2008) is also consistent with our conclusion that OEE is the cause of rare adverse behavioural effects. On the basis of our findings, we do not advocate that oseltamivir treatment be discontinued in young people, but we do suggest that guidelines be developed for safer use of this drug in this particular age group. It should be possible, for example, to develop OEE that does not inhibit MAO-A.

Acknowledgements

We thank Drs. Noriko Echigo and Daigo Sumi for their assistance. This study was supported by the Japan Society for the Promotion of Science (22590422).

Conflicts of interest

Authors declare no competing financial interests.

References

Abdel-Rahman SM, Newland JG, Kearns GL (2011). Pharmacologic considerations for oseltamivir disposition: focus on the neonate and young infant. Paediatr Drugs 13: 19–31.

Bonivento D, Milczek EM, McDonald GR, Binda C, Holt A, Edmondson DE *et al.* (2010). Potentiation of ligand binding through cooperative effects in monoamine oxidase B. J Biol Chem 285: 36849–36856.

Burkard WP, Bonetti EP, Da Prada M, Martin JR, Polc P, Schaffner R *et al.* (1989). Pharmacological profile of moclobemide, a short-acting and reversible inhibitor of monoamine oxidase type A. J Pharmacol Exp Ther 248: 391–399.

Caspi A, McClay J, Moffitt TE, Mill J, Martin J, Craig IW *et al.* (2002). Role of genotype in the cycle of violence in maltreated children. Science 297: 851–854.

Chen K, Holschneider DP, Wu W, Rebrin I, Shih JC (2004). A spontaneous point mutation produces monoamine oxidase A/B knock-out mice with greatly elevated monoamines and anxiety-like behavior. J Biol Chem 279: 39645–39652.

Chung S, Joung YS (2010). Oseltamivir (Tamiflu) induced depressive episode in a female adolescent. Psychiatry Investig 7: 302–304.

Crabb DW, Matsumoto M, Chang D, You M (2004). Overview of the role of alcohol dehydrogenase and aldehyde dehydrogenase and their variants in the genesis of alcohol-related pathology. Proc Nutr Soc 63: 49–63.

Crain SM, Shen KF (2004). Neuraminidase inhibitor, oseltamivir blocks GM1 ganglioside-regulated excitatory opioid receptor-mediated hyperalgesia, enhances opioid analgesia and attenuates tolerance in mice. Brain Res 995: 260–266.

De Clercq E (2006). Antiviral agents active against influenza A viruses. Nat Rev Drug Discov 5: 1015–1025.

Dixon M, Webb EC (1979). Enzymes, 3rd edn. Longman Group Ltd.: London.

Donner B, Bader-Weder S, Schwarz R, Peng MM, Smith JR, Niranjan V (2011). Safety profile of oseltamivir during the 2009 influenza pandemic. Pharmacoepidemiol Drug Saf 20: 532–543.

El-Sayed WM, Al-Kahtani MA (2011). Potential adverse effects of oseltamivir in rats: males are more vulnerable than females. Can J Physiol Pharmacol 89: 623–630.

Freichel C, Breidenbach A, Hoffmann G, Körner A, Gatti S, Donner B *et al.* (2012). Absence of central nervous system and hypothermic effects after single oral administration of high doses of oseltamivir in the rat. Basic Clin Pharmacol Toxicol 111: 50–57.

Furlong RA, Ho L, Rubinsztein JS, Walsh C, Paykel ES, Rubinsztein DC (1999). Analysis of the monoamine oxidase A (MAOA) gene in bipolar affective disorder by association studies, meta-analyses, and sequencing of the promoter. Am J Med Genet 88: 398–406.

Goto J, Kataoka R (2008). ASEDock-Docking based on alpha spheres and excluded volumes. J Chem Inf Model 48: 583–590.

Guzmán DC, García EH, Brizuela NO, Jiménez FT, Mejía GB, Olguín HJ *et al.* (2010). Effect of oseltamivir on catecholamines and select oxidative stress markers in the presence of oligoelements in the rat brain. Arch Pharm Res 33: 1671–1677.

Haley TJ, McCormick WG (1957). Pharmacological effects produced by intracerebral injection of drugs in the conscious mouse. Br J Pharmacol Chemother 12: 12–15.

Hata K, Koseki K, Yamaguchi K, Moriya S, Suzuki Y, Yingsakmongkon S *et al.* (2008). Limited inhibitory effects of oseltamivir and zanamivir on human sialidases. Antimicrob Agents Chemother 52: 3484–3491.

Hatori A, Arai T, Yanamoto K, Yamasaki T, Kawamura K, Yui J *et al.* (2009). Biodistribution and metabolism of the anti-influenza drug [^{11}C]oseltamivir and its active metabolite [^{11}C]Ro 64-0802 in mice. Nucl Med Biol 36: 47–55.

Hatori A, Yui J, Yanamoto K, Yamasaki T, Kawamura K, Takei M *et al.* (2011). Determination of radioactivity in infant, juvenile and adult rat brains after injection of anti-influenza drug [^{11}C]oseltamivir using PET and autoradiography. Neurosci Lett 495: 187–191.

Hirabayashi M, Iwai F, Iizuka M, Mesaki T, Alam MR, Tadokoro S (1979). Individual differences in the accelerating effect of methamphetamine, D-amphetamine and morphine on ambulatory activity in mice. Folia Pharmacol Jpn 75: 683–693.

Iwai Y, Murakami K, Gomi Y, Hashimoto T, Asakawa Y, Okuno Y *et al.* (2011). Anti-influenza activity of marchantins, macrocyclic bisbibenzyls contained in liverworts. PLoS ONE 6: e19825.

Izumi Y, Tokuda K, O'Dell KA, Zorumski CF, Narahashi T (2007). Neuroexcitatory actions of Tamiflu and its carboxylate metabolite. Neurosci Lett 426: 54–58.

Izumi Y, Tokuda K, O'Dell K, Zorumski C, Narahashi T (2008). Synaptic and behavioral interactions of oseltamivir (Tamiflu) with neurostimulants. Hum Exp Toxicol 27: 911–917.

Jefferson T, Demicheli V, Rivetti D, Jones M, Di Pietrantonj C, Rivetti A (2006). Antivirals for influenza in healthy adults: systematic review. Lancet 367: 303–313.

Jefferson T, Jones M, Doshi P, Del Mar C (2009). Neuraminidase inhibitors for preventing and treating influenza in healthy adults: systematic review and meta-analysis. BMJ 339: b5106.

Kadowaki T, Komagamine T, Suzuki K, Hirata K (2011). Oseltamivir-induced dyskinesia in Parkinson's disease. Parkinsonism Relat Disord 17: 133–134.

Kaji M, Fukuda T, Tanaka M, Aizawa H (2005). A side effect of neuraminidase inhibitor in a patient with liver cirrhosis. J Infect Chemother 11: 41–43.

Kamal MA, Greig NH, Alhomida AS, Al-Jafari AA (2000). Kinetics of human acetylcholinesterase inhibition by the novel experimental Alzheimer therapeutic agent, tolserine. Biochem Pharmacol 60: 561–570.

Kishimoto Y, Higashihara E, Fukuta A, Nagao A, Kirino Y (2013). Early impairment in a water-finding test in a longitudinal study of the Tg2576 mouse model of Alzheimer's disease. Brain Res 1491: 117–126.

Kitching A, Roche A, Balasegaram S, Heathcock R, Maguire H (2009). Oseltamivir adherence and side effects among children in three London schools affected by influenza A(H1N1)v, May 2009 – an internet-based cross-sectional survey. Euro Surveill 14: 2–5.

L'Huillier AG, Lorenzini KI, Crisinel PA, Rebsamen MC, Fluss J, Korff CM *et al.* (2011). ABCB1 polymorphisms and neuropsychiatric adverse events in oseltamivir-treated children during influenza H1N1/09 pandemia. Pharmacogenomics 12: 1493–1501.

Lindemann L, Jacobsen H, Schuhbauer D, Knoflach F, Gatti S, Wettstein JG *et al.* (2010). *In vitro* pharmacological selectivity profile of oseltamivir prodrug (Tamiflu) and active metabolite. Eur J Pharmacol 628: 6–10.

McNamara RK, Logue A, Stanford K, Xu M, Zhang J, Richtand NM (2006). Dose–response analysis of locomotor activity and stereotypy in dopamine D3 receptor mutant mice following acute amphetamine. Synapse 60: 399–405.

Maxwell SR (2007). Tamiflu and neuropsychiatric disturbance in adolescents. BMJ 334: 1232–1233.

Medina RA, García-Sastre A (2011). Influenza A viruses: new research developments. Nat Rev Microbiol 9: 590–603.

Meyer JH, Ginovart N, Boovariwala A, Sagrati S, Hussey D, Garcia A *et al.* (2006). Elevated monoamine oxidase a levels in the brain: an explanation for the monoamine imbalance of major depression. Arch Gen Psychiatry 63: 1209–1216.

Moscona A (2005). Neuraminidase inhibitors for influenza. N Engl J Med 353: 1363–1373.

Nakamura K, Schwartz BS, Lindegårdh N, Keh C, Guglielmo BJ (2010). Possible neuropsychiatric reaction to high-dose oseltamivir during acute 2009 H1N1 influenza A infection. Clin Infect Dis 50: e47–e49.

Neumann G, Noda T, Kawaoka Y (2009). Emergence and pandemic potential of swine-origin H1N1 influenza virus. Nature 459: 931–939.

Ose A, Kusuhara H, Yamatsugu K, Kanai M, Shibasaki M, Fujita T *et al.* (2008). P-glycoprotein restricts the penetration of oseltamivir across the blood-brain barrier. Drug Metab Dispos 36: 427–434.

Ose A, Ito M, Kusuhara H, Yamatsugu K, Kanai M, Shibasaki M *et al.* (2009). Limited brain distribution of [3R,4R,5S]-4-acetamido-5-amino-3-(1-ethylpropoxy)-1-cyclohexene-1-carboxylate phosphate (Ro 64-0802), a pharmacologically active form of oseltamivir, by active efflux across the blood-brain barrier mediated by organic anion transporter 3 (Oat3/Slc22a8) and multidrug resistance-associated protein 4 (Mrp4/Abcc4). Drug Metab Dispos 37: 315–321.

Oshima S, Nemoto E, Kuramochi M, Saitoh Y, Kobayashi D (2009). Penetration of oseltamivir and its active metabolite into the brain after lipopolysaccharide-induced inflammation in mice. J Pharm Pharmacol 61: 1397–1400.

Reagan-Shaw S, Nihal M, Ahmad N (2008). Dose translation from animal to human studies revisited. FASEB J 22: 659–661.

Roughan JV, Wright-Williams SL, Flecknell PA (2009). Automated analysis of postoperative behaviour: assessment of HomeCageScan as a novel method to rapidly identify pain and analgesic effects in mice. Lab Anim 43: 17–26.

Sabol SZ, Hu S, Hamer D (1998). A functional polymorphism in the monoamine oxidase A gene promoter. Hum Genet 103: 273–279.

Satoh K, Nonaka R, Ogata A, Nakae D, Uehara S (2007). Effects of oseltamivir phosphate (Tamiflu) and its metabolite (GS4071) on monoamine neurotransmission in the rat brain. Biol Pharm Bull 30: 1816–1818.

Shih JC, Chen K, Ridd MJ (1999). Monoamine oxidase: from genes to behavior. Annu Rev Neurosci 22: 197–217.

Son SY, Ma J, Kondou Y, Yoshimura M, Yamashita E, Tsukihara T (2008). Structure of human monoamine oxidase A at 2.2-Å resolution: the control of opening the entry for substrates/inhibitors. Proc Natl Acad Sci U S A 105: 5739–5744.

Suzuki M, Masuda Y (2008). Effect of a neuraminidase inhibitor (oseltamivir) on mouse jump-down behavior *via* stimulation of dopamine receptors. Biomed Res 29: 233–238.

Takashima T, Yokoyama C, Mizuma H, Yamanaka H, Wada Y, Onoe K *et al.* (2011). Developmental changes in P-glycoprotein function in the blood–brain barrier of nonhuman primates: PET study with R-^{11}C-verapamil and ^{11}C-oseltamivir. J Nucl Med 52: 950–957.

Tarkiainen EK, Backman JT, Neuvonen M, Neuvonen PJ, Schwab M, Niemi M (2012). Carboxylesterase 1 polymorphism impairs oseltamivir bioactivation in humans. Clin Pharmacol Ther 92: 68–71.

Toovey S, Rayner C, Prinssen E, Chu T, Donner B, Thakrar B *et al.* (2008). Assessment of neuropsychiatric adverse events in influenza patients treated with oseltamivir: a comprehensive review. Drug Saf 31: 1097–1114.

Uchiyama H, Toda A, Imoto M, Nishimura S, Kuroki H, Soeda S *et al.* (2010). The stimulatory effects of caffeine with oseltamivir (Tamiflu) on light-dark behavior and open-field behavior in mice. Neurosci Lett 469: 184–188.

Usami A, Sasaki T, Satoh N, Akiba T, Yokoshima S, Fukuyama T *et al.* (2008). Oseltamivir enhances hippocampal network synchronization. J Pharmacol Sci 106: 659–662.

Valley MP, Zhou W, Hawkins EM, Shultz J, Cali JJ, Worzella T *et al.* (2006). A bioluminescent assay for monoamine oxidase activity. Anal Biochem 359: 238–246.

Wang S, Le TQ, Kurihara N, Chida J, Cisse Y, Yano M *et al.* (2010). Influenza virus-cytokine-protease cycle in the pathogenesis of vascular hyperpermeability in severe influenza. J Infect Dis 202: 991–1001.

Yoshino T, Nisijima K, Shioda K, Yui K, Kato S (2008). Oseltamivir (Tamiflu) increases dopamine levels in the rat medial prefrontal cortex. Neurosci Lett 438: 67–69.

Youdim MB, Bakhle YS (2006). Monoamine oxidase: isoforms and inhibitors in Parkinson's disease and depressive illness. Br J Pharmacol 147 (Suppl. 1): S287–S296.

Youdim MB, Edmondson D, Tipton KF (2006). The therapeutic potential of monoamine oxidase inhibitors. Nat Rev Neurosci 7: 295–309.

Zhu HJ, Markowitz JS (2009). Activation of the antiviral prodrug oseltamivir is impaired by two newly identified carboxylesterase 1 variants. Drug Metab Dispos 37: 264–267.

Zhu HJ, Appel DI, Jiang Y, Markowitz JS (2009). Age- and sex-related expression and activity of carboxylesterase 1 and 2 in mouse and human liver. Drug Metab Dispos 37: 1819–1825.

Supporting information

Additional Supporting Information may be found in the online version of this article at the publisher's web-site:

Figure S1 Degradation of neurotransmitters such as dopamine and serotonin by MAO-A and MAO-B, and by aldehyde dehydrogenase. MAOs deaminate monoamines into their aldehyde forms, which are subsequently converted into a carboxylate form by aldehyde dehydrogenase. Both the A and B forms of MAO deaminate dopamine to produce 3,4-dihydroxyphenylacetaldehyde (DOPAldehyde). This compound is subsequently converted into 3,4-dihydroxyphenylacetic acid (DOPAC) by aldehyde dehydrogenase.

Figure S2 *In silico* docking simulation of serotonin with MAO-A. (A) To validate the *in silico* docking simulation, we performed this analysis of MAO-A using serotonin, a known substrate. The results showed that serotonin was fitted into the active pocket of MAO-A. The α-helix and β-strands are shown in red and yellow, respectively. Serotonin is shown here as a ligand and is displayed in a sphere mode. (B) *In silico* two-dimensional analysis of the interaction between serotonin and human MAO-A. The chemical structure of serotonin is shown in the centre with the key interacting amino acids depicted around it. The amino acids and their numbers are indicated. The modes of the interactions are shown.

Figure S3 Schema of injections into the mouse brain and subsequent behavioural analysis shown in Figure 7.

Table S1 Comparison of the Ki & Km values of OEE and other inhibitors and native substrates of MAO-A.

Supporting Information Movies Enhanced spontaneous physical activities (SPA) in mice injected with OEE. These 1-minute-movies show typical behavioural activities in mice from 5 minutes after the intraventricular injection of OEE. These mouse behaviours were recorded by video and analyzed using the HomeCageScan system. Stimulated behaviours were noticeable in OEE-injected mice (OEE1.mov, OEE2.mov, and OEE3.mov). The walk distances in the injected animals were as follows: 2.60, 2.52, and 2.21 m for OEE; 0.64 m for OC (OC.mov); and 0.57 m for the controls (control.mov). The yellow, pink, and cyan lines indicate the edges of the cage. The green line indicates the feeding basket. The very short red line in the centre denotes the faucet of the drinking bottle. The moving grey line shows the mouse body.

Supplementary Information Methods, Discussion and References.